SUPPLEMENTAL INFORMATION

Attenuated adenosine-to-inosine editing of microRNA-376a* promotes invasiveness of glioblastoma cells

Yukti Choudhury[1], Felix Chang Tay[2], Dang Hoang Lam[1,2], Edwin Sandanaraj[3], Carol Tang[4], Beng-Ti Ang[3,4], and Shu Wang[1,2]*

[1]Institute of Bioengineering and Nanotechnology, Singapore
[2]Department of Biological Sciences, National University of Singapore, Singapore
[3]Singapore Institute for Clinical Sciences, Singapore
[4]Department of Neurosurgery and Neuro-Oncology Research Laboratory, National Neuroscience Institute, Singapore

Index of Supplemental Information

SUPPLEMENTAL MATERIAL AND METHODS

RNA isolation

Total RNA from cultured cells, cell pellets or tissue samples was prepared using TRIzol (Invitrogen). For frozen tumor samples, tissues were rapidly homogenized in appropriate volume of TRIzol using an ultrasonic processor (Vibra-Cell, Sonics & Materials). For xenograft tumors, tumor tissue in paraformaldehyde-fixed, OCT-embedded cryosections was separated from normal brain tissue and processed using FFPE RNA Isolation Kit (SA Bioscience) to remove paraformaldehyde cross-links and isolate RNA.

miRNA, siRNA duplexes, LNA, plasmids and transfection

All miRNA duplexes corresponding to miR-376a* were synthesized by Dharmacon. mIRIDIAN microRNA Mimic Negative Control #2 from Dharmacon was used as control miRNA. Two siRNAs against AMFR (SI00022533 and SI00022540) and against RAP2A (SI00128989 and SI03040198) were purchased from Qiagen. Each siRNA targets a distinct region of target mRNA. siGENOME Non-Targeting siRNA #5 from Dharmacon was used as control siRNA. LNA against miR-376a*A and LNA-scr were purchased from Exiqon. Anti-miR miRNA inhibitor against miR-376a* (4464084) and miRNA Inhibitor Negative Control #1 inhibitor were purchased from Ambion.

For stable expression of miRNAs, the Block-iT Pol II miR RNAi expression system (Invitrogen) was used to engineer pre-miRNA cassette to express only miR-376a*. In the stem-loop design, only miR-376a* guide strand is active and passenger strand does not correspond to miR-376a. Briefly, following manufacturer's protocol, the top strand of duplex encoded miR-376a* with "A" or "G" at position 3 of the mature miRNA. The bottom strand sequence followed from the top strand as per protocol of Block-iT kit. The top and bottom strands were annealed and ligated to the linearized pcDNA™6.2-GW/EmGFP-miR vectors to generate pre-miR-376a* plasmids.

For generation of stable U87 cell lines, pmiR-376a*A or G plasmids were transfected using Lipofecatmine 2000. Stable clones were selected over 2 weeks using 6 µg/ml blasticidin (Invitrogen). Four clones were selected and characterized for each construct.

For expression of ADARB1, pCMV-SPORT6-ADARB1 was purchased from Open Biosystem. pCMV-SPORT6-EGFP was constructed by inserting EGFP coding sequence between EcoRV and NotI sites of pCMV-SPORT6. The miR-376 cluster expression vector was constructed using the Block-iT Pol II miR RNAi system where the pcDNA™6.2-GW/EmGFP vector was first recircularized using a 20 bp linker sequence, and the genomic region corresponding miR-376 cluster was amplified from human genomic DNA and inserted between SalI and BglII sites using the following primers: 5'-ATGTCGACGAGAGTGATGGAAGGT-3' and 5'-ATAGATCTATACTGAGAACACAGCCTTG-3'.

For luciferase reporter assay, pMir-Report was purchased from Ambion. For construction of RAP2A and AMFR 3'UTR reporter plasmids, 3'UTR regions were amplified from human genomic DNA and

inserted into into SpeI and MluI sites for AMFR full length and AMFR-417, SacI and PmeI sites for RAP2A-2475 and HindIII and MluI site for RAP2A-1154.

For expression of RAP2A- and AMFR–ORF only, expression constructs were purchased from GeneCopoeia (EX-A0400-M68 for RAP2A and EX-T9295-M68 for AMFR). Full-length expression constructs including 3'UTR were purchased from Origene (SC113011 for RAP2A and SC119417 for AMFR). A control vector was generated by Not I digestion and recircularization of pCMV6-XL4-containing full-length RAP2A. Co-transfection of expression constructs (400 ng DNA) and miRNA duplexes (50 nM per well of 6-well plates) was done with Lipofectamine 2000.

miRNA mimics (Dharmacon) were transfected at concentration of 10 - 50 nM in glioma cells using Lipofectamine RNAiMax. Similarly, siRNAs (Dharmacon or Qiagen) were transfected at 1 - 10 nM concentration. Locked-nucleic acid (LNA) and Anti-miR miRNA inhibitor transfection was done at 50 nM using Lipofectamine RNAiMax.

Wound healing and invasion assay

For wound healing assay, cells were cultured in 6-well plates, transfected and allowed to reach confluence. An artificial homogenous wound was made using a sterile p200 tip. For comparison of parental U87 cells and ELM-selected U87 cells, $1X10^5$ cells were seeded in 6-well plates and allowed to reach confluence before scratches were made as described. Cell debris was removed by washing cells with DPBS and medium was replaced with 1% FBS-containing DMEM. The wound borders were imaged just after wounding (t = 0 h) and again after 24 or 36 hours to measure the wound gap distance. Wound coverage was determined as percentage of the gap width covered during incubation.

For in vitro invasion assay, the Boyden chamber assay with Matrigel-coated inserts with 8-µm pores was used (BD Falcon). Three days after transfection with 10 nM miRNA, 2.5 nM siRNA, or with mixture of plasmid DNA and miRNA, glioma cells were starved overnight in unsupplemented OPTI-MEM (Invitrogen). On the day of the assay, cells were stained with Calcein-AM (Invitrogen), trypsinized and seeded onto the upper chamber ($1X10^5$ cells in 200 µl of unsupplemented OPTI-MEM media). Lower chambers were filled with 700 µl of supplemented OPTI-MEM (10% FBS). After 24 hours of incubation at 37ºC, fluorescence readings of invaded cells at the bottom of inserts were measured with Victor3 1420 Multilabel Counter (Perkin Elmer) or number of labeled invading cells was manually counted from 4-5 imaged fields.

Cell viability, proliferation, and cell cycle assays

Cell viability was measured in 96-well plates using the Cell-Titer Glo Assay (Promega). For growth rate assessment of stable U87 cells or parental and ELM-selected cells, 3000 cells were seeded per well of 96-well plates. Viability was measured from day 0 (day of seeding) until day 7.

Cell proliferation was quantified using the colorimetric BrdU cell proliferation assay (Roche). Briefly, at indicated times after transfection, cells were labeled with BrdU for 12 hrs. Labeled cells were fixed and

BrdU incorporation was measured as per the protocol using the anti-BrdU-peroxidase immunodetection. Absorbance of the colored product was measured at 370 nm (reference wavelength 492 nm) in a microplate reader (Bio-Rad).

For cell cycle analysis, cells treated as indicated were trypsinized and fixed in ice-cold 70% ethanol. Fixed cells were resuspended in PBS containing 0.1% Triton X-100, 20 µg/ml propidium iodide and 200 µg/ml RNase A and incubated in the dark for 30 minutes before analysis by flow cytometry (Beckman Coulter).

Luciferase reporter assay

For luciferase reporter assay, HeLa cells in 96-well plates were transfected with 30 ng of reporter plasmid, 30 ng of CMV-ß-galactosidase and 20 nM miRNA mimics using Lipofectamine 2000. After 48 hours, luciferase activity was measured using the Luciferase Assay system (Promega). Luciferase readings were normalized to ß-galactosidase activity in the same lysate, quantified by the ß-galactosidase Enzyme Assay System (Promega).

Immunohistochemistry

Immunohistochemical detection was done on paraformaldehyde-fixed, OCT-embedded cryosections. Following heat-induced antigen retrieval in citrate buffer, sections were incubated with mouse anti-Ki-67 antibody (1:100 dilution, Dako) and rabbit anti-vWF antibody (prediluted, Abcam). Where fluorescent detection was done, Alex-Fluor 568 conjugated secondary antibodies (1:200 dilution, Molecular Probes) were used. For immunoperoxidase staining, biotin-conjugated secondary antibodies (1:200 dilution, BD Biosciences) were used in a three-step detection protocol (Millipore). DAB substrate was from BD Biosciences. Quantification of fluorescent Ki-67 signal was done using NIH ImageJ, by first converting images to 8-bit, subtracting background and adjusting threshold range to 17-255 (1). Signal intensities were enumerated from similar-size fields (5-6 fields for each tumor core or tumor edge) of different images and compared.

Western blotting and immunocytochemistry

Protein lysates were prepared 72 hours after transfection using Cellytic M (Sigma) buffer. Protease inhibitor (Fermentas) was added to the lysis buffer at appropriate concentrations. Protein was quantified by DC protein assay (Bio-Rad). Twenty to forty micrograms of protein was separated on SDS-PAGE and transferred to nitrocellulose membrane using the iBlot system (Invitrogen). Membrane was blocked with 5% BSA and incubated overnight with rabbit anti-RAP2A (1:1000, GeneTex), rabbit anti-AMFR (1:5000, Novus Biologicals) and mouse anti-ß-actin (1:2000, Abcam). Horseradish peroxidase (HRP)-conjugated anti-mouse secondary antibody (Abcam) was used at 1:2000 dilution and HRP-conjugated anti- rabbit secondary antibody (Amersham) was used at 1:5000 dilution. Chemiluminescent detection of protein was done using Amersham ECL Plus (GE Healthcare) and band intensities were quantified using ImageJ.

Immunostaining of actin cytoskeleton in methanol-acetone fixed cells was done using FITC-conjugated anti-actin antibody (1:500, Abcam).

Microarray and bioinformatics analyses

Total RNA from U87 and SW1783 cell lines transfected as indicated was isolated using Trizol. For each cohort, three independent RNA samples were isolated. Following clean-up with Qiagen RNeasy column, amplification and labeling was done by Kreatech ULS labeling kit as per protocol. Fifteen µg of each labeled RNA sample was hybridized to Affymetrix Human Genome U133 Plus 2.0 arrays. CEL files were imported into GeneSpring GX 11 (Agilent) and signal intensities normalized using MAS5 algorithm and processed to remove 'absent' probesets and those in the lowest 20th percentile from analysis. Genes were filtered based on 1.5- or 2-fold change and $P < 0.05$, with respect to their respective control experiments. Enrichment of specific GO biological functions among the differentially expressed genes was evaluated by NCBI DAVID bioinformatics analysis (http://david.abcc.ncifcrf.gov/) using default settings. For miRNA binding site prediction, RNA 22 analysis (http://cbcsrv.watson.ibm.com/rna22.html) (2) was done on whole 3'UTR sequences and miR-376a* sequence with "A" or "G".

Survival analysis in public glioma datasets

We evaluated the survival association of mRNA expression for target genes in 2 independent public glioma patient datasets, REMBRANDT and "Gravendeel". The probesets were mapped to target genes by annotating the gene expression datasets with Affymetrix annotation (v32). The gene expression of patients was subdivided into two classes according to the expression level of individual genes. The patients who had gene expression values greater than and less than median expression of individual gene were classified as high-expression and low-expression groups, respectively. The survival time for the REMBRANDT dataset was scaled from months to years to provide a consistent representation across the 2 datasets. Kaplan-Meier survival curves were plotted for each subgroup of glioma patients. The difference among the survival curves was estimated using the generalized log-rank test. Results with log-rank test p-values of less than 0.05 were considered statistically significant. The probeset mapping and survival analysis (3) were performed using R software packages called affy and survival, respectively (http://cran.rproject.org/web/packages/survival/index.html).

Reverse-transcription PCR

Real-time PCR quantification of mature miRNAs was done as described previously (4) except the sequence of the poly (T) adaptor used for cDNA synthesis was modified to 5'-CGATAGCGACGATACAGACTTGTCACTATAGG(T)12VN*-3' and sequence of reverse primer was: 5'-CGATAGCGACGATACAGACTTG-3'. The forward primers corresponded to the full length mature miRNA sequence and were as follows:

miR-376a*A: 5'- GTAGATTCTCCTTCTATGAGTAAA

miR-376a*G: 5’- GTGGATTCTCCTTCTATGAGTAAA
miR-376a: 5’- ATCATAGAGGAAAATCCACGTAAA
miR-376b: 5’- ATCATAGAGGAAAATCCATGTTAAA
miR-376a2-5p: 5’- GTAGATTTTCCTTCTATGGTTAAA
miR-376c: 5’-ACATAGAGGAAATTCCACGTAAA
miR-127: 5’- TCGGATCCGTCTGAGCTTGGCTAAA
miR-154: 5’- TAGGTTATCCGTGTTGCCTTCGAAA
miR-432: 5’- TCTTGGAGTAGGTCATTGGGTTGGAAA
miR-654: 5’- TGGTGGGCCGCAGAACATGTGCAAA
miR-16: 5’-TAGCAGCACGTAAATATTGGCGAAA
miR-21: 5’-TAGCTTATCAGACTGATGTTGAAA
miR-221: 5’-AGCTACATTGTCTGCTGGGTTTCAAA
miR-106: 5’-AAAAGTGCTTACAGTGCAGGTAGAAA
miR-10b: 5’-TACCCTGTAGAACCGAATTTGTGAAA

5S rRNA was used as an internal control. For comparison of miRNA expression in normal brain and tumor tissue, miR-16 was used for normalization (5). We determined that both A and G-containing primers were able to amplify miR-376a* with similar efficiencies by real-time PCR using SYBR-Green PCR Mix (Applied Biosystems). For real-time PCR of mRNAs, total RNA was reverse transcribed using random hexamers by Superscript III RT-PCR kit (Invitrogen). Resulting cDNA was used for PCR using SYBR-Green PCR Mix. PCR and data collection was done on Bio-Rad iCycler Bio-Rad. Expression levels were normalized to 18S rRNA. RT-PCR for primary miRNAs was done using random hexamer cDNAs and primers used in primary miRNA editing analysis.

Oligonucleotide Sequences

PCR and sequencing primers for primary miRNA editing analysis:

Primary miRNA	Size (bp)	Forward	Reverse
pri-miR-376a1	159	5’-acaggtgcacgctttcct-3’	5’-tccatggcgacttcacgt-3’
pri-miR-376a2	159	5’-ggattgtacttaggttcgtgc-3’	5’-tggcttcagtccagccat-3’
pri-miR-376b	166	5’-ccatgaactgtgttcagatttg-3’	5’-ctacggtctcttccagaaac-3’
pri-miR-376c	154	5’-gatagattgtgcttaggttcatgc-3’	5’-gtccaggaatgtttccaagc-3’

Adapters and primers for cloning mature miR-376 cluster RNAs:

5’ RNA adapter: 5' -CGACUGGAGCACGAGGACACUGACAUGGACUGAAGGAGUAGAAA -3'

RT adapter for small RNA cDNA library synthesis: 5'-ATTCTAGAGGCCGAGGCGGCCGACATG-d(T)30 VN-3'

FW primer: 5'-CTGACATGGACTGAAGGA-3'

miR-376c RV primer: 5'-TAAACGTGGAATTTCCTC-3'

miR-376a1-5p RV primer: 5'- CAGCACTCATAGAAGGA -3'

miR-376a/b RV primer: 5'-TTTTWACRTGGATTTTCCTC-3' (R= A or G, W= A or T)

miR-376a2-5p RV primer: 5'- CACGTAACCATAGAAGG-3'

Oligonucleotide sequences for Block-iT pri-miR-376a* and control miRNA expression plasmid:

pri-miR-376a*A:

Top: 5'-TGCTGGTAGATTCTCCTTCTATGAGTAGTTTTGGCCACTGACTGACTACTCATAAGGAGAATCTAC-3'

Bottom:

5'-

CCTGGTAGATTCTCCTTATGAGTAGTCAGTCAGTGGCCAAAACTACTCATAGAAGGAGAATCTACC-3'

pri-miR-376a*G:

Top:

5'-TGCTGGTGGATTCTCCTTCTATGAGTAGTTTTGGCCACTGACTGACTACTCATAAGGAGAATCCAC-3'

Bottom:

5'-

CCTGGTGGATTCTCCTTATGAGTAGTCAGTCAGTGGCCAAAACTACTCATAGAAGGAGAATCCACC-3'

cel-miR-239b:

Top:

5'TGCTGTTGTACTACACAAAAGTACTGGTTTTGGCCACTGACTGACCAGTACTTGTGTAGTACAA3'

Bottom:

5'CCTGTTGTACTACACAAGTACTGGTCAGTCAGTGGCCAAAACCAGTACTTTTGTGTAGTACAAC 3'

Primers for 3'UTR cloning:

3'UTR	Size of PCR product (bp)	Forward	Reverse
RAP2A-2475	2475	agctGAGCTCCATCCAAATATGGCT	agtcGTTTAAACCACATTCATTTGCCA
RAP2A-1154	1154	acgtACGCGTCATCCAAATATGGCT	tgcaAAGCTTGCTTTTGTCCCTTAC
RAP2A-426	426	tgacGAGCTCTGTTAGTGAATTGGT	agtcGTTTAAACCACATTCATTTGCCA
AMFR full length	1411	tcgtACTAGTCGCTCCCTTGCCTTCCT	atgcACGCGTTAGCTATGCTCTCAGCA
AMFR-417	417	tgctACTAGTGTGTGAACCTACCTGCC	atgcACGCGTTAGCTATGCTCTCAGCA

qRT-PCR primers for mRNAs:
Primer set for ADAR and ADARB1 were purchased from SA Biosciences.

Gene	Forward	Reverse
RAP2A	TTCCAGGTCCACTTTGTTCC	AGCAGAGCTTCCAGGACATC
AMFR	TTCCTACACAGCGGTCAGATAGC	GCCGAAGTCCAGCGTCTCC
PDGFRα	CCACCGTCAAAGGAAAGAAG	CCAATTTGATGGATGGGACT
PDGFRβ	CAGGAGAGACAGCAACAGCA	AACTGTGCCCACACCAGAAG
PDGFα	GATACCTCGCCCATGTTCTG	CAGGCTGGTGTCCAAAGAAT
PDGFβ	TCGAGTGGTCACTCAGCATC	GCGCTCTTCCTGTCTCTCTG
VEGFA	AGCCTTGCCTTGCTGCTCTA	GTGCTGGCCTTGGTGAGG
TGFβR1	TTGTCTTTTGTACAGAGGTGGC	GCTGCTCCTCCTCGTGCT
TGFβR2	GGAAACTTGACTGCACCGTT	CTGCACATCGTCCTGTGG
TGFα	GGGCAGTCATTAAAATGGGA	GCTCTGGGTATTGTGTTGGC
TGFβ1	CTTCCAGCCGAGGTCCTT	CCCTGGACACCAACTATTGC
TGFβ2	CTCCATTGCTGAGACGTCAA	ATAGACATGCCGCCCTTCTT
EGFR	TCCTCTGGAGGCTGAGAAAA	GGGCTCTGGAGGAAAAGAAA
ANGPT1	CCGACTTCATGTTTTCCACA	ACCGGATTTCTCTTCCCAGA
ANGPTL2	GGTAGATGGAGCTGGTGTCG	CACTATGCCCACTCTCACCA
ANGPTL4	TAGTCCACTCTGCCTCTCCC	GAGATGGCCCAGCCAGTT
CXCL12	TGGGCTCCTACTGTAAGGGTT	TTGACCCGAAGCTAAAGTGG
CXCR4	TTTTCTTCACGGAAACAGGG	GTTACCATGGAGGGGATCAG
ITGB3	TCATCAGAGCACCAGGCA	TCTGGGCGACTGTGCTG
FN1	ACCTCGGTGTTGTAAGGTGG	CCATAAAGGGCAACCAAGAG
HIF1α	TGGCTGCATCTCGAGACTTT	GAAGACATCGCGGGGAC
NTNG1	GGGTACTCGCATCACACTCA	AAGTGAAACTCGATCCTCCG
TNXB	TCTCAGCTTCATTTCCGTGA	TCTACGGGAGCACAGTGGAC
MMP2	GGAAAGCCAGGATCCATTTT	ATGCCGCCTTTAACTGGAG
PLAU	CCAGCTCACAATTCCAGTCA	TGACCCACAGTGGAAAACAG
HGF	CCCTGTAGCCTTCTCCTTGA	CGCTGGGAGTACTGTGCAAT
NRP2	TGCTCCAGTCCACCTCGTAT	AACTGCATGGAACCCATCTC
18S rRNA	AACTTTCGATGGTAGTCGCCG	CCTTGGATGTGGTAGCCGTTT

SUPPLEMENTAL REFERENCES

1. Feuer R, Pagarigan RR, Harkins S, Liu F, Hunziker IP, Whitton JL. Coxsackievirus targets proliferating neuronal progenitor cells in the neonatal CNS. *J Neurosci.* 2005;25(9):2434-2444.

2. Miranda KC, Huynh T, Tay Y, et al. A pattern-based method for the identification of MicroRNA binding sites and their corresponding heteroduplexes. *Cell.* 2006;126(6):1203-1217.

3. Harrington DP, Fleming TR. A class of rank test procedures for censored survival data. *Biometrika.* 1982;69:553-566.

4. Wu C, Lin J, Hong M, et al. Combinatorial control of suicide gene expression by tissue-specific promoter and microRNA regulation for cancer therapy. *Mol Ther.* 2009;17(12):2058-2066.

5. Gabriely G, Yi M, Narayan RS, et al. Human Glioma Growth Is Controlled by MicroRNA-10b. *Cancer Res.* 2011;71(10):3563-3572.

Figure S1

A

miRNA	Fold-change in GBM	p-value
miR-376a*	0.853	2.49E-05
miR-376a	0.517	1.18E-09
miR-376b	0.941	0.0422
miR-376c	0.789	8.54E-05

B

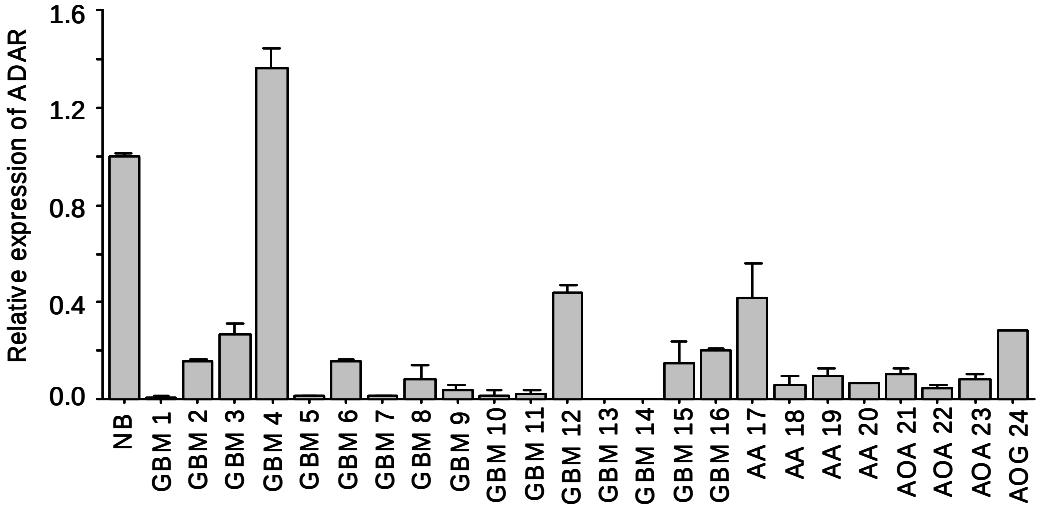

C

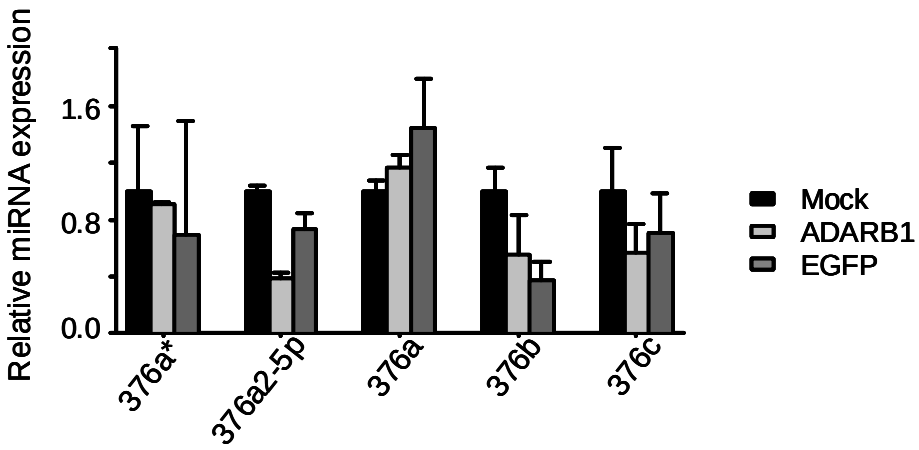

Supplemental Figure 1. A-to-I editing of miR-376 cluster is reduced in glioma

(A) Summary of data analysis of the Cancer Genome Atlas using Anduril framework for miRNA expression in GBMs. Samples used for the analysis include 251 GBMs. Fold-change is relative to miRNA expression in 10 normal brain samples. P-values associated to fold change are obtained from the same analysis.

(B) Relative expression levels of editing enzyme *ADAR* mRNA by qRT-PCR in normal brain (NB) and tumor samples (n = 3). All values were normalized to 18S rRNA levels in the same sample.

(C) Relative expression by qRT-PCR of endogenous mature miR-376a*, miR-376a2-5p, miR-376a, miR-376b and miR-376c in U87 cells transfected with ADARB1 or EGFP expression plasmids (n = 3).

Error bars indicate SD.

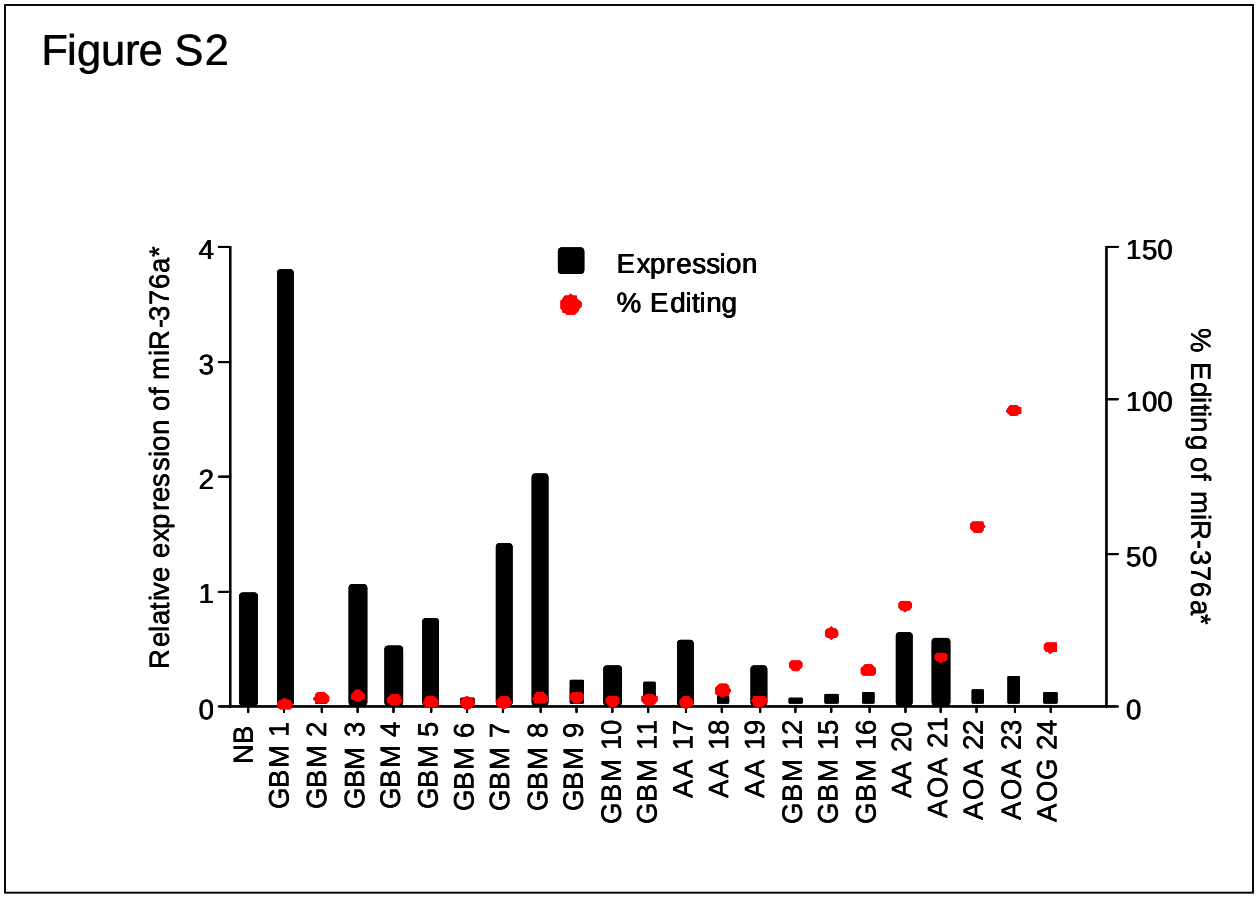

Supplemental Figure 2. Accumulation of unedited miR-376a* correlates with glioma invasion.

Expression of total miR-376a* in tumor samples measured by qRT-PCR. Values were normalized to miR-16 (n = 3). % Editing of miR-376a* in the same sample is also indicated.

Figure S3

A

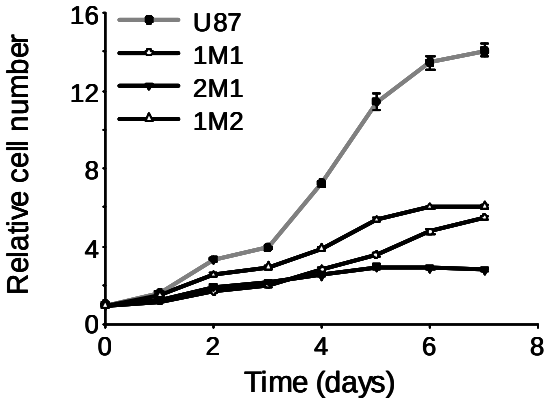

B

Frequency of Editing (%)

	pri-miR-376a1			pri-miR-376a2			pri-miR-376b	pri-miR-376c	
Cell line	site +5	+9 ‡	+44	+11	+15	+55	+67	+4	+48
U87	1.61	3.6	4.69	11.23	14.62	75.74	52.61	0.96	42.69
1M1	1.68	5.82	5.02	20.5	19.82	78.55	61.72	1.02	42.78
1M2	2.11	3.89	7.02	14.91	13.89	69	55.75	3.95	30.69
2M1	2.28	2.85	7.31	10.54	15.93	74.66	56.14	1.7	36.73

Supplemental Figure 3. Editing and expression of miR-376 cluster in invasive glioma cells

(A) In vitro growth curves for parental U87 and ELM-selected cells. For each cohort, number of cells in five wells was counted for 7 days as indicated and plotted relative to cell number on day 0. Data represents mean ± SD.

(B) Quantification of editing frequencies for miR-376 cluster editing sites in U87 and ELM cells by direct sequencing of RT-PCR products of primary miRNAs (pri-miRs). For each pri-miR, the 5' end of stem-loop sequence annotated in the Sanger miRBase site is counted as +1. Editing frequency is calculated as the % ratio of G peak over the sum of A and G peaks for the editing site.

Figure S4

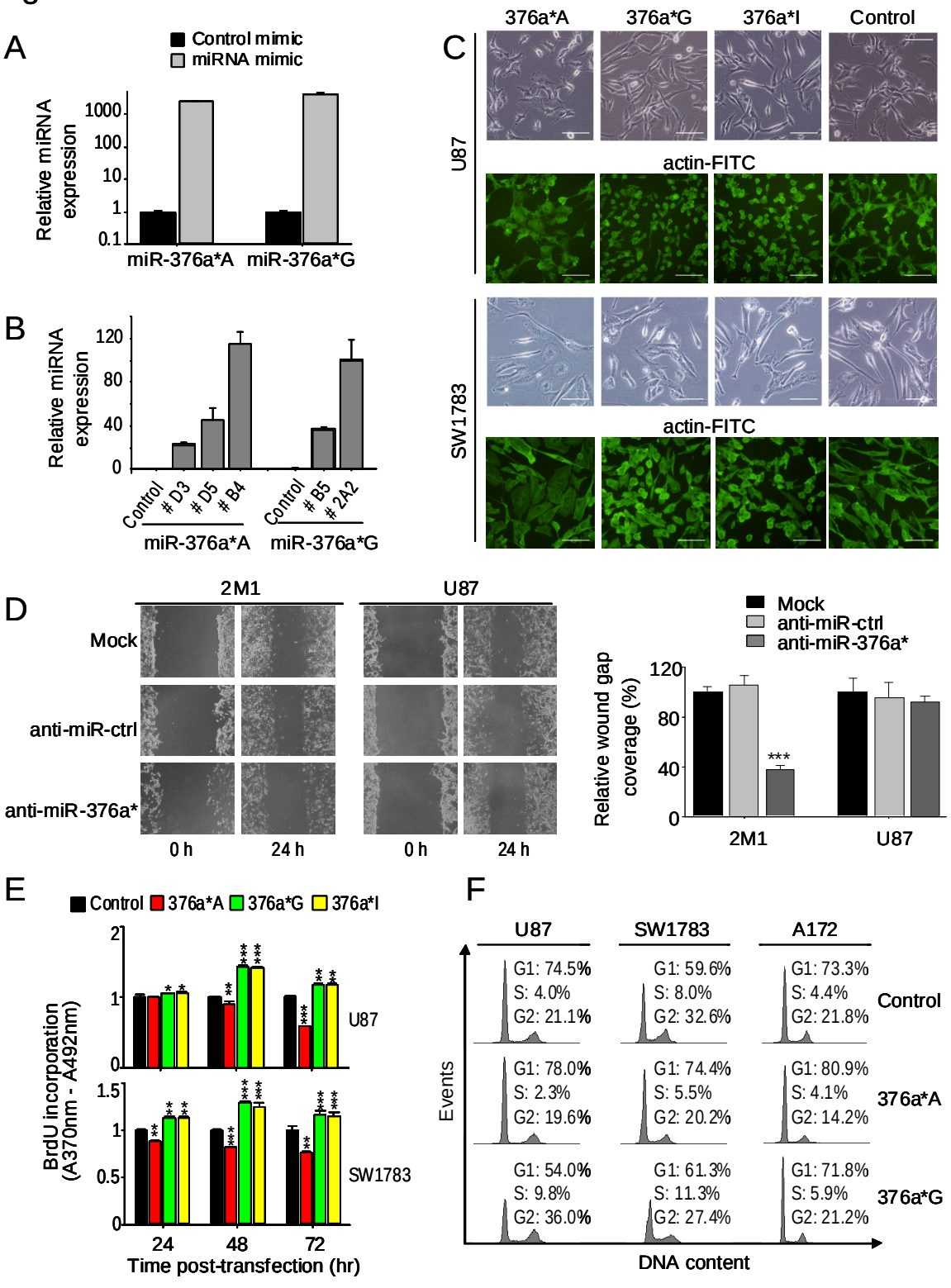
A
Control mimic
miRNA mimic
Relative miRNA expression
1000
100
10
1
0.1
miR-376a*A
miR-376a*G
B
Relative miRNA expression
120
80
40
0
Control
D3
D5
B4
Control
B5
2A2
miR-376a*A
miR-376a*G
C
376a*A
376a*G
376a*I
Control
U87
actin-FITC
SW1783
actin-FITC
D
2M1
U87
Mock
anti-miR-ctrl
anti-miR-376a*
0 h
24 h
0 h
24 h
Mock
anti-miR-ctrl
anti-miR-376a*
Relative wound gap coverage (%)
120
80
40
0
***
2M1
U87
E
Control
376a*A
376a*G
376a*I
BrdU incorporation (A370nm - A492nm)
2
1
0
U87
1.5
1
0.5
0
SW1783
24
48
72
Time post-transfection (hr)
F
U87
SW1783
A172
G1: 74.5%
S: 4.0%
G2: 21.1%
G1: 59.6%
S: 8.0%
G2: 32.6%
G1: 73.3%
S: 4.4%
G2: 21.8%
Control
G1: 78.0%
S: 2.3%
G2: 19.6%
G1: 74.4%
S: 5.5%
G2: 20.2%
G1: 80.9%
S: 4.1%
G2: 14.2%
376a*A
G1: 54.0%
S: 9.8%
G2: 36.0%
G1: 61.3%
S: 11.3%
G2: 27.4%
G1: 71.8%
S: 5.9%
G2: 21.2%
376a*G
Events
DNA content

Supplemental Figure 4. Unedited miR-376a* promotes glioma cell invasion in vitro

(A) Expression of miR-376a*A or miR-376a*G in U87 cells transiently transfected with 10 nM miRNA mimics. Measurement was done by qRT-PCR using forward primers corresponding to A- or G- version of miR-376a* (n = 3). Values were normalized to 5S rRNA levels in the same sample.

(B) Expression of miR-376a*A in stably transfected U87 cell lines D3, D5, and B4, and miR-376a*G expression in stably transfected U87 cell lines B5 and 2A2 (n = 3). Values were normalized to 5S rRNA levels in the same sample.

(C) Morphology of U87 and SW1783 glioma cells transiently transfected with miR-376a*A/G/I or control miRNA. Actin-FITC labeling highlights the organized actin cytoskeleton in miR-376a*A transfected cells. Loss of cytoskeletal organization can be observed in both miR-376a*G and miR-376a*I transfected cells. Scale bar = 60 µm.

(D) Wound healing migration assay of U87 cells and ELM-selected 2M1 cells after anti-miRNA inhibitor-mediated knockdown of miR-376a*A. anti-miR-ctrl : miRNA against control (n = 3).

(E) Measurement of relative proliferation rates of transiently transfected U87 and SW1783 cells, using the BrdU incorporation assay. BrdU incorporation was measured at indicated time-points after transfection and five wells were used for each group.

(F) Flow cytometry to assess cell cycle distribution of transfected U87, A172 and SW1783 glioma cells. While miR-376a*A causes an increase in cells in G1 phase, miR-376a*G results in an increase in cells in S- and G2/M-phases. Percentage of cells in each phase was quantified by using CellQuest software (Becton Dickinson) and is shown as mean. Representative traces from 3 different experiments are shown. Error bars indicate SD. *$p < 0.05$, **$p < 0.01$, ***$p < 0.001$ by t test.

Supplemental Table 1. Summary of DAVID functional enrichment analysis for differentially expressed genes in miR-376a*-transfected U87 cells, identified by Affymetrix microarray

Annotated Biological Process†	Enrichment Score	p-value	FDR	Gene Count	%
Genes up-regulated by miR-376a*A					
GO:0007275~multicellular organismal development	15.20	3.8E-21	6.9E-18	199	29.3
GO:0001944~vasculature development	8.50	6.3E-11	1.1E-07	35	5.2
GO:0007155~cell adhesion	8.17	2.0E-11	3.6E-08	65	9.6
GO:0001501~skeletal system development	6.44	2.9E-09	5.3E-06	37	5.4
GO:0030154~cell differentiation	5.82	2.8E-12	5.0E-09	117	17.2
GO:0006928~cell motion	5.29	4.9E-07	8.8E-04	42	6.2
GO:0009605~response to external stimulus	4.81	9.5E-10	1.7E-06	73	10.8
Genes down-regulated by miR-376a*A					
GO:0022403~cell cycle phase	4.06	1.5E-06	2.7E-03	42	4.7
GO:0044248~cellular catabolic process	2.22	3.8E-04	6.7E-01	70	7.9
Genes up-regulated by miR-376a*G					
GO:0007049~cell cycle	35.13	1.6E-47	2.8E-44	166	13.7
GO:0006259~DNA metabolic process	10.54	2.1E-28	3.8E-25	105	8.7
GO:0000226~microtubule cytoskeleton organization	8.64	1.8E-11	3.2E-08	35	2.9
GO:0051726~regulation of cell cycle	7.81	9.5E-16	1.8E-12	64	5.3
GO:0007059~chromosome segregation	7.68	2.9E-17	5.2E-14	32	2.6
Genes down-regulated by miR-376a*G					
GO:0001944~vasculature development	6.59	4.4E-09	7.9E-06	44	3.6
GO:0009653~anatomical structure morphogenesis	4.47	1.6E-07	2.9E-04	124	10.1
GO:0009966~regulation of signal transduction	4.15	8.9E-07	1.6E-03	95	7.8
GO:0030154~cell differentiation	2.73	5.2E-05	9.4E-02	146	11.9
GO:0016477~cell migration	2.37	5.2E-04	9.5E-01	34	2.8

† List of transcripts that had were up- or down-regulated >2-fold, P value <0.05, 72 hours after treatment with miR-376a*A or miR-376a*G relative to control miRNA were analyzed for enrichment of GO biological processes using DAVID Bioinformatics Resources. The most significantly enriched GO Biological Process annotation terms in the gene lists, are presented with enrichment score, p-value, false discovery rate, the number and % of total genes falling in each annotation cluster. p-value of enrichment modified Fisher's exact test.

Figure S5

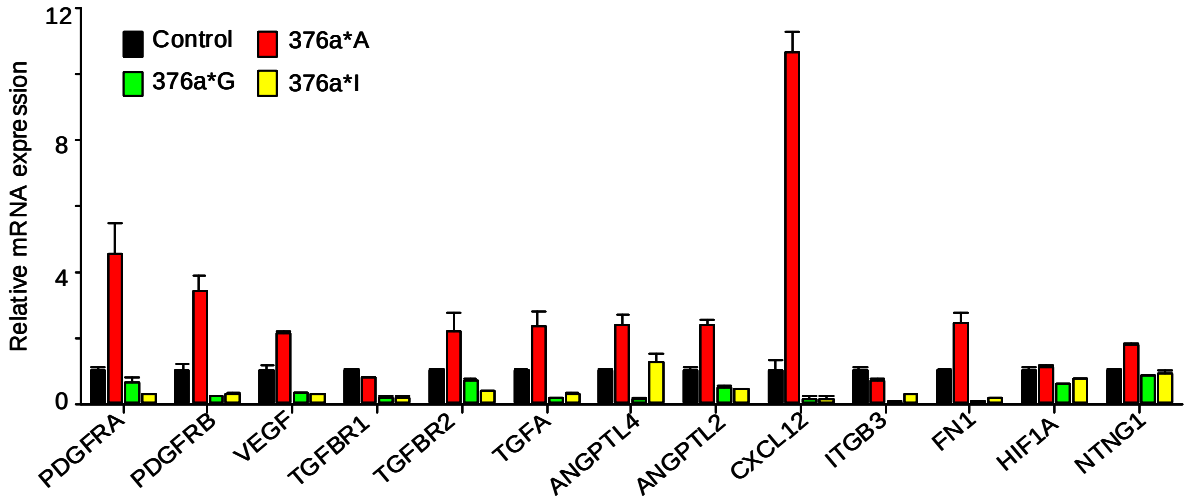

Supplemental Figure 5. Expression of invasion-related genes is similarly modulated by miR-376a*G and miR-376a*I.

Expression verification by qRT-PCR of genes involved in glioma migration, invasion and angiogenesis in U87 cells transfected with miR-376a*A/G/I (n = 3). Expression was normalized to 18S rRNA.

Figure S6

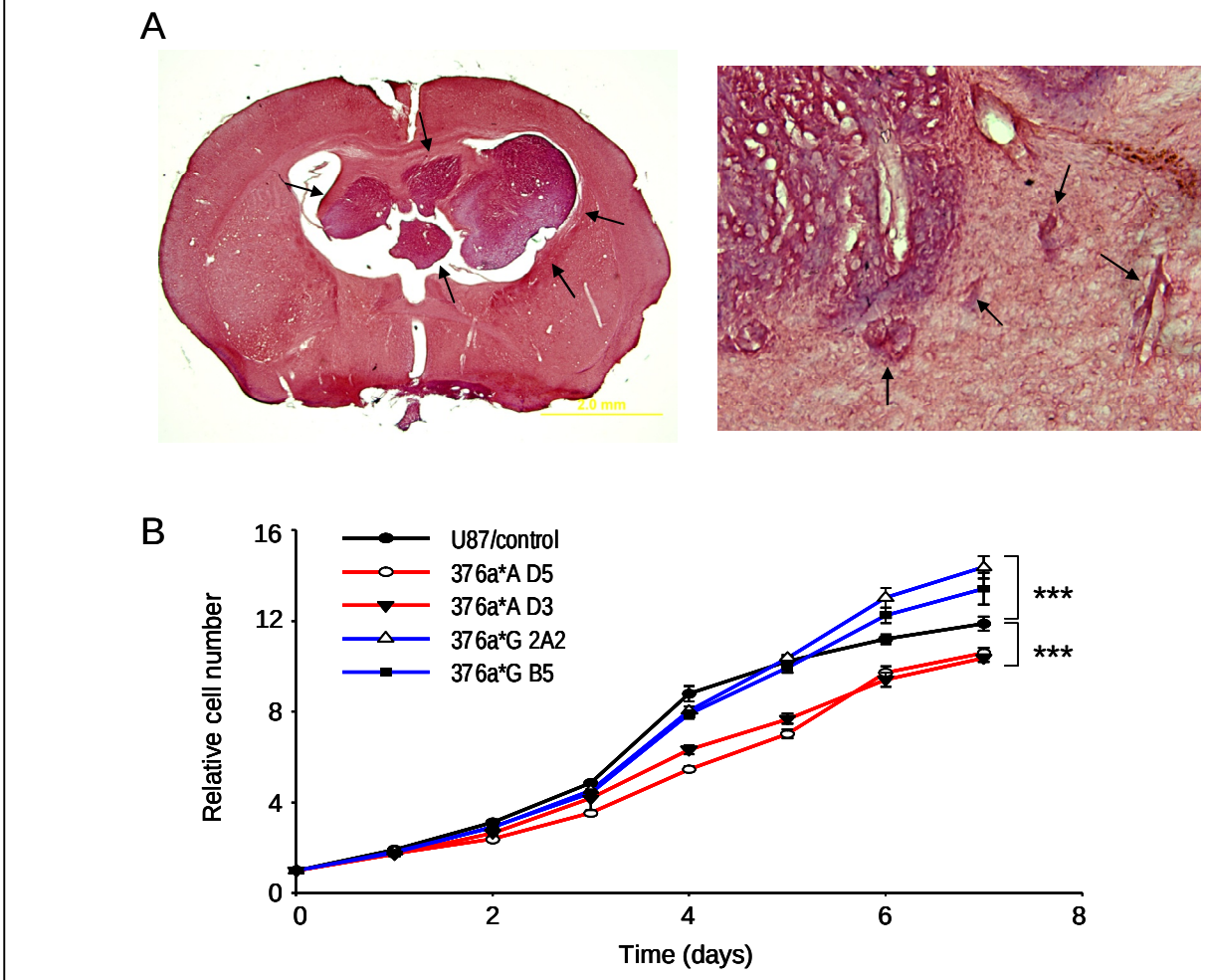

Supplemental Figure 6. Unedited miR-376a* promotes glioma cell invasion in vivo

(A) H&E staining of tumor sections from the B4 clone of U87 cell line stably transfected with miR-376a*A. *Left*: H&E staining showing the formation of disseminated tumors after intrastratum injection of B4 cells. Arrows indicate tumor foci; *Right*: H&E staining showing irregular tumor boundary at higher magnification and tumor satellites (arrows). Scale bar: 200 μm.

(B) In vitro growth curves of U87 cells stably transfected with miR-376a*A (red curves), miR-376a*G (blue) or control miRNA (black). For each cohort, number of cells in five wells was counted for 7 days as indicated and plotted relative to cell number on day 0.

Error bars indicate SD. ***p < 0.001 by t test.

Figure S7

A

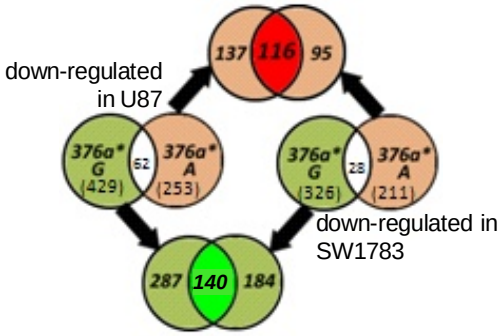

B

```
miR-376a*A  3'→5'  AUG--AGUAUCUUCCUCUUAGAUG   AU---GAGUAUCUUCCUCUUAGAUG
                      ||  ||||   :|:|||:|:|       |||         | ||||:|
   H. sapiens      GGCTGTCCTGGAT--GGGATTTGC   TCAGTCTCCTTTAT---GCATCTGC
   P. troglodytes  GGCTGTCCTGGAT--GGGATTTGC   TCAGTCTCCTTTAT---GCATCTGC
   M. mulatta      GGCTGTCCTGGAT--GGGATTTGC   TCAGTCTCCTTTAT---GCATCTGC
   B. taurus                                  TCAGTCcCCTccAT---GCAcCTGC
   M. musculus                                TCAGTCcttgta------CATCTGC
RAP2A 3'UTR 5'→3'          nt 12-33                  nt 203-224

miR-376a*A  3'→5'  AUGAGUAUCUUCCUCUUAGAUG    AUGAGUAUCUU-CC----UCUUAGAUG
                      |||||      :||||||         ||||   ||    |||||:|::
   H. sapiens      AAGGCATAGTCCATCGATCTAC    -----ATAGTCTGGCTTTAGAATTTGT
   P. troglodytes  AAGGCATAGTCCATCGATCTAC    -----ATAGTCTGGCTTTAGAATTTGT
   M. mulatta      AAGGCATAGTCCATCGATCTAC    -----ATAGTCTGGCTTTAGAATTTGT
   B. taurus                                 -----AcAGcCTGatgTTAGAA--TGT
   M. musculus                               -----ccAGtCTGGCTTTAGAATcTGT
RAP2A 3'UTR 5'→3'          nt 231-252                nt 660-681

miR-376a*A  3'→5'  AUGAGUAUCUUCC-UCUUAGAUG   A--UGAGUAU-CUUCCUCUUAGAUG
                    :||:          ||  ||:|:|     ||  |||: |||    |||:|:
   H. sapiens      -GCTTTCAAAATCAAGTATTTGC   ATAAC-CATGTGAAAT--AATTTGG
   P. troglodytes  -GCTTTCAAAATCAAGTATTTGC   ATAAC-CATGTGAAAT--AATTTGG
   M. mulatta      -GCTTTCAAAATCAAGT--TTGC   ATAAC-CATGTGAAAT--AATTTGG
   B. taurus       -GCTTTCAAAATCAAGT--TTtC   ATAAC-CATGTGAAAT--AA-TTGG
   M. musculus
RAP2A 3'UTR 5'→3'          nt 1026-1047              nt 1085-1106
```

C

```
miR-376a*G  3'→5'  AU--GAGUAUCUUCCUCUUAGGUG   AUGAGUAUCUUCC----UCU---UAGGUG
                      |||  |||||  ||||||||         |||||     ||    ||||||
   H. sapiens      AGTCCTTTTGGGA--AGAATCCAG   -------GGAAGAATCCAGTATTATCCAC
   P. troglodytes  AGTCCTTTTGGGA--AGAATCCAG   -------GGAAGAATCCAGTATTATCtAC
   M. mulatta      AGTCCTTTTGGGA--AGAATCCAG   -------GGAAGAATCCAGTATTATCtAC
   C. familiaris   AGTCCTTTTGGGA--AGAATCCAG   -------GGAAGAATCCAGTATTATCtAa
   M. musculus     AGTCCTTTTGGGA--AaAATCCAG   -------GGAAAAATCCAGTATTATCtAa
AMFR 3'UTR 5'→3'           nt 1183-1204              nt 1192-1214
```

Supplemental Figure 7. Distinct target gene specificities of unedited and edited miR-376a*

(A) Schematic diagram for identification of target genes that are uniquely regulated by either miR-376a*A or miR-376a*G. Numbers of transcripts down-regulated in response to overexpression of miR-376a*A or 376a*G in U87 and SW1783 cells are included. Numbers of transcripts exclusively down-regulated by miR-376a*A in both cell lines are presented in the area shaded red and those corresponding to miR-376a*G in the area shaded green. These represent candidate target genes for each miRNA.

(B) Alignment of potential miR-376a*A-binding sites in *RAP2A* 3'UTRs of different species indicating evolutionary conservation.

(C) Alignment of potential miR-376a*G-binding sites in *AMFR* 3'UTRs of different species indicating evolutionary conservation.

Supplemental Table 2. Genes downregulated by miR-376a*A in U87 and SW1783 cells*

Symbol	Description	Fold-change in U87	Fold-change in SW1783
SEPT10	septin 10	2.38	2.04
ADAM17	ADAM metallopeptidase domain 17	1.77	1.64
ALG2	asparagine-linked glycosylation 2, alpha-1,3-mannosyltransferase homolog (S. cerevisiae)	2.37	1.91
ARL6	ADP-ribosylation factor-like 6	3.32	2.72
ARMCX5	armadillo repeat containing, X-linked 5	4.70	2.63
ATP10D	ATPase, class V, type 10D	1.92	1.81
B3GAT3	beta-1,3-glucuronyltransferase 3 (glucuronosyltransferase I)	2.09	2.04
BAG5	BCL2-associated athanogene 5	1.72	1.66
BRI3BP	BRI3 binding protein	4.32	3.28
BZW1	basic leucine zipper and W2 domains 1	3.24	3.27
C18orf54	chromosome 18 open reading frame 54	2.42	2.29
C18orf55	chromosome 18 open reading frame 55	2.43	2.09
C7orf58	chromosome 7 open reading frame 58	2.02	2.00
CAST	calpastatin	1.76	1.60
COMMD2	COMM domain containing 2	6.03	4.08
DENR	density-regulated protein	1.67	1.77
DIP2A	DIP2 disco-interacting protein 2 homolog A (Drosophila)	2.13	2.03
DKFZP564C152	DKFZP564C152 protein		
DPYD	dihydropyrimidine dehydrogenase	2.68	1.91
ELOVL5	ELOVL family member 5, elongation of long chain fatty acids (FEN1/Elo2, SUR4/Elo3-like, yeast)	4.80	2.30
EPB41L5	erythrocyte membrane protein band 4.1 like 5	1.58	1.65
ERLIN2	ER lipid raft associated 2	2.80	1.93
FAM168A	family with sequence similarity 168, member A	2.56	1.98
FAM18B	family with sequence similarity 18, member B	4.79	4.45
FAM20B	family with sequence similarity 20, member B	1.67	1.60
FAM55C	family with sequence similarity 55, member C	3.16	2.38
FGF2	fibroblast growth factor 2 (basic)	2.63	3.52
FRMD5	FERM domain containing 5	1.74	1.77
G3BP2	GTPase activating protein (SH3 domain) binding protein 2	3.11	2.07
GALNT11	UDP-N-acetyl-alpha-D-galactosamine:polypeptide N-acetylgalactosaminyltransferase 11 (GalNAc-T11)	2.03	1.57
GFPT1	glutamine-fructose-6-phosphate transaminase 1	2.82	2.09
GIGYF2	GRB10 interacting GYF protein 2	1.97	1.62
GLT8D3	glycosyltransferase 8 domain containing 3	1.70	1.96
GNE	glucosamine (UDP-N-acetyl)-2-epimerase/N-acetylmannosamine kinase	2.03	1.94
GOLPH3L	golgi phosphoprotein 3-like	1.88	1.71
HDAC9	histone deacetylase 9	2.34	1.87
HNRNPAB	heterogeneous nuclear ribonucleoprotein A/B	2.05	1.73
ISOC1	isochorismatase domain containing 1	2.77	2.31
KCTD12	potassium channel tetramerisation domain containing 12	2.69	2.65
KDSR	3-ketodihydrosphingosine reductase	4.52	2.88
KIF16B	kinesin family member 16B	2.85	2.99
KPNA6	karyopherin alpha 6 (importin alpha 7)	1.99	1.86
LARS2	leucyl-tRNA synthetase 2, mitochondrial	1.67	1.70
LOC643287	similar to prothymosin alpha	2.54	2.70
LOC727914	BMS1-like, ribosome assembly protein (yeast) pseudogene	3.14	2.05
LRRFIP2	leucine rich repeat (in FLII) interacting protein 2	1.52	1.66
LYRM7	Lyrm7 homolog (mouse)	1.72	1.57
MAP2	microtubule-associated protein 2	1.57	1.75
MDH1	malate dehydrogenase 1, NAD (soluble)	2.41	1.91
MED28	Mediator complex subunit 28	4.09	2.00
MELK	maternal embryonic leucine zipper kinase	3.14	2.79
MIS12	MIS12, MIND kinetochore complex component, homolog (yeast)	2.05	1.98
MLF1IP	MLF1 interacting protein	2.97	1.81
MUS81	MUS81 endonuclease homolog (S. cerevisiae)	1.61	1.54
MYH9	myosin, heavy chain 9, non-muscle	1.97	1.68
NAPG	N-ethylmaleimide-sensitive factor attachment protein, gamma	3.49	2.98
NHLRC3	NHL repeat containing 3	2.84	1.99
NSUN2	NOL1/NOP2/Sun domain family, member 2	2.47	2.32
NUDT15	nudix (nucleoside diphosphate linked moiety X)-type motif 15	2.55	2.30

NUP50	nucleoporin 50kDa	2.45	1.77
ORAI3	ORAI calcium release-activated calcium modulator 3	2.23	2.11
PANK4	pantothenate kinase 4	1.85	1.82
PEX19	peroxisomal biogenesis factor 19	5.12	3.34
PIP4K2A	phosphatidylinositol-5-phosphate 4-kinase, type II, alpha	2.59	2.07
PITRM1	pitrilysin metallopeptidase 1	3.48	3.14
POMGNT1	protein O-linked mannose beta1,2-N-acetylglucosaminyltransferase	2.38	2.27
PPP2R2A	protein phosphatase 2 (formerly 2A), regulatory subunit B, alpha isoform	1.51	1.61
PTPRJ	protein tyrosine phosphatase, receptor type, J	1.57	2.10
RAB8B	RAB8B, member RAS oncogene family	2.78	2.91
RAP2A†	**RAP2A, member of RAS oncogene family**	**1.75**	**1.60**
RAPGEF6	Rap guanine nucleotide exchange factor (GEF) 6	1.63	1.77
RBM17	RNA binding motif protein 17	1.82	1.50
RNF138	ring finger protein 138	1.67	1.61
RNF141	ring finger protein 141	2.68	2.20
RPS6KA3	ribosomal protein S6 kinase, 90kDa, polypeptide 3	1.97	2.28
RPS6KB1	ribosomal protein S6 kinase, 70kDa, polypeptide 1	3.22	2.63
RRAS2	related RAS viral (r-ras) oncogene homolog 2	6.26	5.37
RSPRY1	ring finger and SPRY domain containing 1	3.30	2.78
RTN4	reticulon 4	1.59	2.07
SCML1	sex comb on midleg-like 1 (Drosophila)	3.68	2.62
SEC23B	Sec23 homolog B (S. cerevisiae)	7.96	5.73
SKP2	S-phase kinase-associated protein 2 (p45)	4.54	1.75
SLC25A43	solute carrier family 25, member 43	3.24	2.62
SLC2A14	solute carrier family 2 (facilitated glucose transporter), member 14	2.57	1.79
SLC35A1	solute carrier family 35 (CMP-sialic acid transporter), member A1	1.98	2.12
SLC38A1	solute carrier family 38, member 1	2.38	1.74
SLC39A10	solute carrier family 39 (zinc transporter), member 10	3.87	3.55
SLC7A11	solute carrier family 7, (cationic amino acid transporter, y+ system) member 11	2.12	1.85
SLC7A6OS	solute carrier family 7, member 6 opposite strand	1.87	2.37
SMN1	survival of motor neuron 1, telomeric	2.72	2.47
SNRPA1	small nuclear ribonucleoprotein polypeptide A'	2.82	1.97
SQSTM1	sequestosome 1	1.82	1.85
STAT3	signal transducer and activator of transcription 3 (acute-phase response factor)	1.84	1.66
SUB1	SUB1 homolog (S. cerevisiae)	1.91	1.88
TDG	thymine-DNA glycosylase	3.24	2.60
THUMPD1	THUMP domain containing 1	1.99	1.89
TOR1B	torsin family 1, member B (torsin B)	4.52	4.73
TPK1	thiamin pyrophosphokinase 1	2.81	2.64
TTC39C	tetratricopeptide repeat domain 39C	2.18	1.70
UGCG	UDP-glucose ceramide glucosyltransferase	2.05	2.22
USP53	ubiquitin specific peptidase 53	1.98	2.03
VEZT	vezatin, adherens junctions transmembrane protein	4.00	3.62
VMA21	VMA21 vacuolar H+-ATPase homolog (S. cerevisiae)	4.63	3.35
VTA1	Vps20-associated 1 homolog (S. cerevisiae)	1.85	1.54
WDR37	WD repeat domain 37	1.99	1.78
YPEL5	yippee-like 5 (Drosophila)	1.81	1.71
YRDC	yrdC domain containing (E. coli)	3.82	2.87
ZCCHC10	zinc finger, CCHC domain containing 10	3.14	2.21
ZFYVE26	zinc finger, FYVE domain containing 26	1.66	2.20
	Full length insert cDNA clone ZB81B12	3.94	3.39
	Full-length cDNA clone CS0DK008YI09 of HeLa cells Cot 25-	6.82	3.88

normalized of Homo sapiens (human)		
CDNA FLJ30661 fis, clone DFNES2000526	4.84	2.77
Homo sapiens, clone IMAGE:4294444, mRNA	1.71	1.56
Full-length cDNA clone CS0DF022YM06 of Fetal brain of Homo sapiens (human)	1.70	1.71
MRNA; cDNA DKFZp586F1523 (from clone DKFZp586F1523)	1.65	1.73
CDNA FLJ30010 fis, clone 3NB692000154	2.26	2.83

*: Transcripts downregulated exclusively by miR-376a*A in both U87 and SW1783 glioma cells (1.5-fold, $p < 0.05$), 24 hours after transfection with miR-376a*A compared to control miRNA are listed. This list resulted after transcripts identified to be commonly downregulated by miR-376a*A and miR-376a*G after similar analysis were excluded (Supplemental Figure 7A).

† RAP2A was selected as candidate target gene of miR-376a*A based on presence of six miR-376a*A binding sites in its 3'UTR as predicted by RNA22, conservation of 3'UTR sites in mammals (Supplemental Figure 7B), and Gene Ontology analysis listing 'negative regulation of cell migration' as a biological process regulated by RAP2A.

Supplemental Table 3. Genes downregulated by miR-376a*G in U87 and SW1783 cells*

Symbol	Description	Fold-change in U87	Fold-change in SW1783
AASDHPPT	aminoadipate-semialdehyde dehydrogenase-phosphopantetheinyl transferase	2.27	2.03
ABHD2	abhydrolase domain containing 2	2.50	2.10
ABL1	c-abl oncogene 1, receptor tyrosine kinase	4.05	3.50
ACVR1	activin A receptor, type I	4.85	4.42
AFF1	AF4/FMR2 family, member 1	1.71	1.58
AFG3L2	AFG3 ATPase family gene 3-like 2 (yeast)	1.88	1.96
AHCYL2	S-adenosylhomocysteine hydrolase-like 2	1.68	1.54
AMFR†	**autocrine motility factor receptor**	**1.9**	**1.71**
AP3M1	adaptor-related protein complex 3, mu 1 subunit	3.51	2.50
APC	adenomatous polyposis coli	2.16	2.03
ARF1	ADP-ribosylation factor 1	2.70	2.11
ARHGAP21	Rho GTPase activating protein 21	3.05	2.54
ARHGAP26	Rho GTPase activating protein 26	2.17	2.21
ARHGEF7	Rho guanine nucleotide exchange factor (GEF) 7	1.52	1.67
ARL4C	ADP-ribosylation factor-like 4C	1.96	1.55
ARMC8	armadillo repeat containing 8	2.23	2.37
ARNTL	aryl hydrocarbon receptor nuclear translocator-like	2.29	1.67
ARRDC3	arrestin domain containing 3	3.02	2.44
BRD3	bromodomain containing 3	1.66	1.56
C10orf26	chromosome 10 open reading frame 26	3.78	2.56
C13orf23	chromosome 13 open reading frame 23	1.97	1.76
C15orf57	chromosome 15 open reading frame 57	3.27	3.06
C17orf39	chromosome 17 open reading frame 39	1.84	1.87
C17orf80	chromosome 17 open reading frame 80	2.15	1.72
C19orf2	chromosome 19 open reading frame 2	1.75	1.59
C1orf96	chromosome 1 open reading frame 96	1.90	1.53
C2orf64	chromosome 2 open reading frame 64	1.77	1.90
C5orf51	chromosome 5 open reading frame 51	3.08	1.81
C9orf126	chromosome 9 open reading frame 126	2.26	1.69
CASP7	caspase 7, apoptosis-related cysteine peptidase	1.90	2.04
CBLB	Cas-Br-M (murine) ecotropic retroviral transforming sequence b	1.81	1.50
CDC26	cell division cycle 26 homolog (S. cerevisiae)	3.21	3.01
CHD6	chromodomain helicase DNA binding protein 6	1.92	1.79
CYB5R4	cytochrome b5 reductase 4	3.79	2.52
DHTKD1	dehydrogenase E1 and transketolase domain containing 1	2.25	1.83
DPYSL3	dihydropyrimidinase-like 3	2.46	3.90
DUSP14	dual specificity phosphatase 14	2.01	1.77
EML4	echinoderm microtubule associated protein like 4	2.04	2.16
EMP2	epithelial membrane protein 2	2.55	1.62
EZH1	enhancer of zeste homolog 1 (Drosophila)	1.88	1.60
FAM120B	Family with sequence similarity 120B	3.13	2.53
FAM122B	family with sequence similarity 122B	2.95	3.91
FAM171A1	family with sequence similarity 171, member A1	2.34	1.94
FBXO46	F-box protein 46	1.89	1.54
FNIP2	folliculin interacting protein 2	2.71	2.45
FOXJ3	forkhead box J3	1.57	1.52
FZD5	frizzled homolog 5 (Drosophila)	2.52	2.53
GAS2L3	Growth arrest-specific 2 like 3	2.11	1.55
GDAP1	ganglioside-induced differentiation-associated protein 1	2.11	1.94
GLOD4	glyoxalase domain containing 4	2.43	2.54
GPR157	G protein-coupled receptor 157	3.50	3.04
GPR180	G protein-coupled receptor 180	1.56	2.01
GRK5	G protein-coupled receptor kinase 5	1.80	2.09

HDAC4	histone deacetylase 4	4.37	2.83
HIPK2	homeodomain interacting protein kinase 2	2.21	1.74
HRSP12	heat-responsive protein 12	3.13	2.47
IL6R	interleukin 6 receptor	2.33	2.44
IMPA2	inositol(myo)-1(or 4)-monophosphatase 2	2.40	2.26
IRGQ	immunity-related GTPase family, Q	2.46	1.79
IRS1	insulin receptor substrate 1	1.68	1.53
JMJD6	jumonji domain containing 6	1.96	1.68
JOSD1	Josephin domain containing 1	2.9	2.31
KIAA2018	KIAA2018	2.25	1.84
KIF1B	kinesin family member 1B	2.48	2.31
KIRREL	kin of IRRE like (Drosophila)	4.10	3.44
KLF13	Kruppel-like factor 13	1.70	2.00
LMAN2L	lectin, mannose-binding 2-like	1.74	1.68
LMLN	leishmanolysin-like (metallopeptidase M8 family)	2.5	3.96
LOC149832	hypothetical protein LOC149832	2.10	2.11
LPP	LIM domain containing preferred translocation partner in lipoma	1.73	1.61
LRRC58	leucine rich repeat containing 58	2.44	2.12
MALT1	mucosa associated lymphoid tissue lymphoma translocation gene 1	3.08	3.17
MAP2K4	mitogen-activated protein kinase kinase 4	1.63	1.53
MCC	mutated in colorectal cancers	1.93	1.66
MED14	mediator complex subunit 14	2.25	1.97
MLXIP	MLX interacting protein	2.61	1.84
MOBKL1B	MOB1, Mps One Binder kinase activator-like 1B (yeast)	2.35	2.06
MYCBP	c-myc binding protein	1.98	1.95
NAV1	neuron navigator 1	3.10	2.38
NRN1	neuritin 1	2.55	1.53
NUCKS1	nuclear casein kinase and cyclin-dependent kinase substrate 1	2.32	1.79
OXSR1	oxidative-stress responsive 1	1.94	2.21
PAFAH1B1	platelet-activating factor acetylhydrolase, isoform Ib, subunit 1 (45kDa)	1.81	1.61
PDLIM5	PDZ and LIM domain 5	1.69	1.56
PEG10	paternally expressed 10	2.54	2.41
PI4K2A	phosphatidylinositol 4-kinase type 2 alpha	1.77	1.51
PLS1	plastin 1 (I isoform)	4.12	3.21
PPFIA1	protein tyrosine phosphatase, receptor type, f polypeptide (PTPRF), interacting protein (liprin), alpha 1	2.18	1.87
PRICKLE2	prickle homolog 2 (Drosophila)	1.84	1.55
PRKAB2	protein kinase, AMP-activated, beta 2 non-catalytic subunit	1.65	1.76
PRKACB	protein kinase, cAMP-dependent, catalytic, beta	2.45	2.11
PRNP	prion protein	1.83	1.66
PRRC1	proline-rich coiled-coil 1	2.78	2.07
PRSS23	Protease, serine, 23	1.81	1.57
PSEN1	presenilin 1	2.27	2.18
PTCH1	patched homolog 1 (Drosophila)	2.45	1.94
RAB31	RAB31, member RAS oncogene family	1.7	2.11
RBM23	RNA binding motif protein 23	2.66	2.05
SCLY	selenocysteine lyase	3.27	1.94
SEC22B	SEC22 vesicle trafficking protein homolog B (S. cerevisiae)	2.95	2.88
SETBP1	SET binding protein 1	1.61	1.68
SLC1A1	solute carrier family 1 (neuronal/epithelial high affinity glutamate transporter, system Xag), member 1	2.56	1.78
SLC30A6	solute carrier family 30 (zinc transporter), member 6	4.93	4.07
SLC38A7	solute carrier family 38, member 7	3.48	2.47
SNX21	sorting nexin family member 21	2.06	2.05
SOCS3	suppressor of cytokine signaling 3	1.71	2.08
ST5	suppression of tumorigenicity 5	2.41	1.69
SYT1	synaptotagmin I	2.59	2.25
TCF7	transcription factor 7 (T-cell specific, HMG-box)	4.58	3.16
TFG	TRK-fused gene	1.77	1.58
TMEM183A	transmembrane protein 183A	4.26	2.51
TMEM33	transmembrane protein 33	3.12	2.82

TNFRSF10B	tumor necrosis factor receptor superfamily, member 10b	2.37	2.37
TNFRSF21	tumor necrosis factor receptor superfamily, member 21	2.30	1.71
TPRG1L	tumor protein p63 regulated 1-like	3.59	2.42
TRIM69	tripartite motif-containing 69	2.26	1.73
TTC7B	tetratricopeptide repeat domain 7B	3.06	1.94
TWSG1	twisted gastrulation homolog 1 (Drosophila)	3.21	1.52
UBE2I	Ubiquitin-conjugating enzyme E2I (UBC9 homolog, yeast)	3.25	3.28
UBE2Z	ubiquitin-conjugating enzyme E2Z	2.01	1.66
UBP1	upstream binding protein 1 (LBP-1a)	3.23	2.21
UFM1	ubiquitin-fold modifier 1	1.62	1.83
UNC13B	unc-13 homolog B (C. elegans)	1.86	1.65
WAPAL	wings apart-like homolog (Drosophila)	2.28	2.10
WBP4	WW domain binding protein 4 (formin binding protein 21)	1.63	1.75
XPNPEP3	X-prolyl aminopeptidase (aminopeptidase P) 3, putative	1.64	2.21
YIPF6	Yip1 domain family, member 6	2.75	2.75
ZAK	sterile alpha motif and leucine zipper containing kinase AZK	1.78	1.82
ZCCHC24	zinc finger, CCHC domain containing 24	1.79	2.19
ZDHHC5	zinc finger, DHHC-type containing 5	2.56	1.98
ZNF23	zinc finger protein 23 (KOX 16)	2.00	2.10
ZNF271	zinc finger protein 271	1.86	2.5
ZNF317	zinc finger protein 317	2.57	1.75
ZNF35	zinc finger protein 35	2.87	1.75
ZXDB	zinc finger, X-linked, duplicated B	1.81	1.88
	CDNA FLJ30652 fis, clone DFNES2000011	2.10	1.87
	CDNA FLJ39585 fis, clone SKMUS2006633	2.54	1.79
	CDNA FLJ31233 fis, clone KIDNE2004579	1.57	1.62
	CDNA FLJ37302 fis, clone BRAMY2016009	1.85	1.78
	CDNA FLJ34250 fis, clone FCBBF4000529	2.23	1.54

* Transcripts downregulated exclusively by miR-376a*G in both U87 and SW1783 glioma cells (1.5-fold, $p < 0.05$), 24 hours after transfection with miR-376a*G compared to control miRNA are listed. This list resulted after transcripts identified to be commonly downregulated by miR-376a*A and miR-376a*G after similar analysis were excluded (Supplemental Figure 7A).

† AMFR was selected as a candidate target gene of miR-376a*G/I based on the prediction of two miR-376a*G binding sites in its 3'UTR and absence of predicted target sites for miR-376a*A, conservation of target sites in mammals (Supplemental Figure 7C) and its known function as a specific receptor for autocrine motility factor (AMF), a tumor motility-stimulating protein secreted by tumor cells.